STATIC AND CYCLIC MODEL PILE TESTS IN SAND

1.4

Dr ir Shigeo Kanai, Geotop Corporation, Tokyo, Japan
Prof. Dr ir William Van Impe, Director Laboratory Soil Mechanics, Ghent University, Belgium.

SYNOPSIS

Model pile tests have been performed in a medium dense dry sand under static compression and one-way cyclic compression loading modes in a pressurized chamber. This paper mainly examines two main parameters affecting the pile behaviour under cyclic loading : pile surface roughness (rough and smooth) and pile installation method (displacement by jacking and buried). Soil strength parameters testing in the deposit by CPT en DMT is also briefly discussed.

INTRODUCTION

An experimental study of the load-settlement behaviour of a model pile in sand, in a calibration chamber (CC), and subjected to static and dynamic loading was performed at Ghent University by the main author. The goal was to clarify, at least qualitatively, the fundamental mechanism of cyclic pile-soil interaction behaviour, focussing on the pile shaft friction mobilisation. Major previous suggestions, Ina (1992) - fig. 1 a,b,c, were mainly related to cohesive soils. The tests described have refer to pure dry quartz sands.

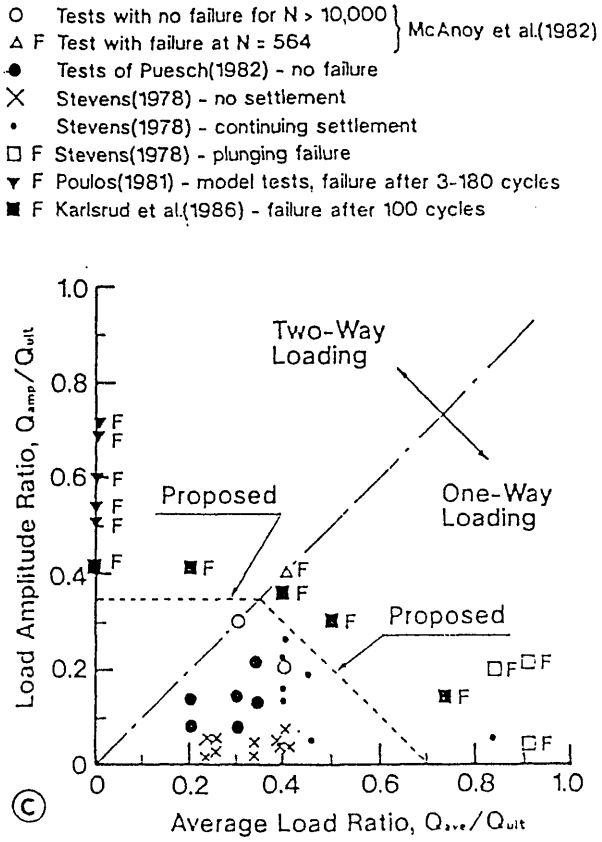

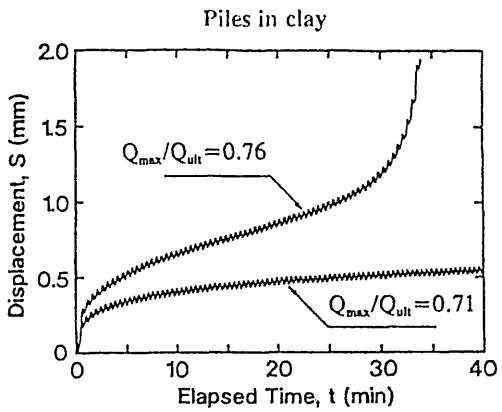

ⓐ alminium pile : d=19 mm, l=374 mm
jacked into sandy clay in CC
T=28 s

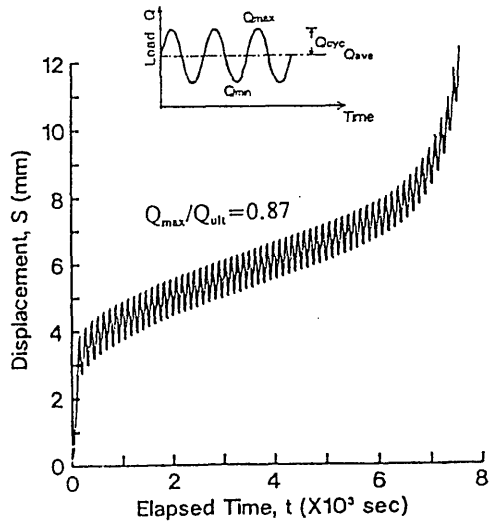

ⓑ steel pile : d=191 mm, l=11.3 m
driven into NC silty clay
T=120 s

Fig. 1 Cyclic loading tests result (Ina 1992)

EQUIPMENT AND TEST PROCEDURE

Fig. 2 shows the setup of the pile loading test. CPT tests are also carried out on identical sand specimens in the CC. Each sand specimen has a 1,4 m effective diameter instrumented ring system and 2.1 m effective height. The ring system was removed in the lateron tests, because of handling difficulties.

The specimen is vertically loaded by 4 oil jacks on the rigid top plate. This overburden pressure is kept constant throughout the test. The model pile or penetrometer is jacked by means of a loading frame mounted on a reaction beam.

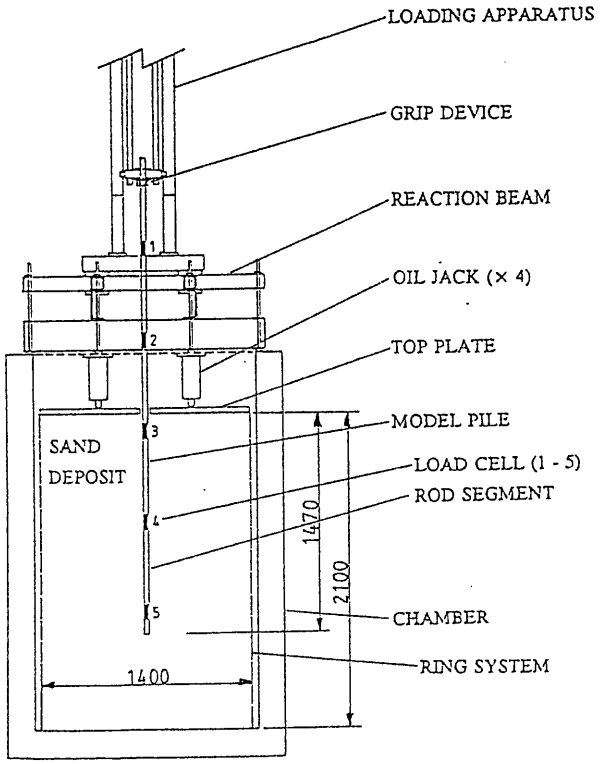

Fig. 2 Pile loading tests setup

The steel top plate has 5 holes : one at centre for pile loading test or cone penetration test. There are also 4 side holes located as shown in this figure. Dilatometer tests and some cone penetration tests were performed out of the centre.

The sand specimens were prepared by a carefull layered tamping method using the undercompaction principle. An amount of sand, equivalent to 0.11 to 0.12 m of the heightfor each layer, is discharged as evenly as possible through a flexible tube. The tube has a set of perforated plates in its tip so that the sand drops on a previous layer in loose condition irrespectively of the drop height. After flattening smoothly the surface of the layer, it is tamped in a severely standardised way and procedure by a rod of 9 kg and diameter 0,30 m. The achieved relative density of the overall sample becomes about 65 % and is very reproducible.

In order to identify the initial state of the specimen, penetration tests, CPT ; DMT ; and LSCT, were conducted in the chamber. The results also provide information of the representative strength and deformation properties of the specimen. The test conditions are assembled in table 1. No notable influence on the results of different location, different side boundary, different rate and loading history was observed.

Table 1 : Summary of the penetration tests

Test No.	D_r (%)	Test location		Chamber boundary		v_p (mm/s)	Remarks
		centre	side	flexible	rigid		
CPT 1	67	O	O	O		12	
CPT 2	67	O	O	O		16	
CPT 3	59	O		O		20	after DMT 2
CPT 4	67		O		O	20	after SD 2 pile test
CPT 5	65		O		O	20	after SD 3 pile test
CPT 6	65		O		O	20	after SD 4 pile test
CPT 7	66		O		O	20	after SD 5 pile test
CPT 8	68		O		O	20	after SND 2 pile test
CPT 9	69		O		O	20	after RND 1 pile test
DMT 1	65		O	O		15	
DMT 2	59		O	O		20	tangential orientation
DMT 3	64		O	O		20	
DMT 4	65		O	O		20	with RD pile installation
DMT 5	68		O		O	20	with SND 3 pile test
LSCT 1	71	O		O		26	
LSCT 2	70	O		O		23	25 cm pre-penetration
LSCT 3	69	O		O		20	5 cm pre-penetration
D_r : relative density						v_p : penetration rate	

Some cone penetration test results are shown in fig. 3. The cone resistance q_c is quickly developed and reaches some plateau in between 0.4-1.6 m of depth. Those constant q_c values correspond very well to the indicated relative density, and ranges between 11-14 MPa. The local skin friction f_l value also corresponds to the expected values but tends to increase slightly with depth.

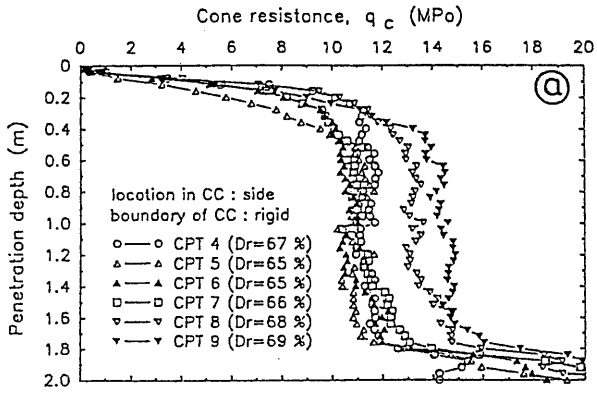

Fig. 3 CPT results

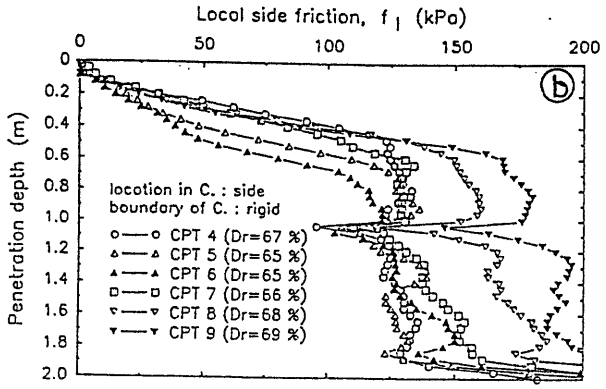

Fig. 3 CPT results

The discontinuities at 1 m of depth are due to the stopping of the test for installing a second CPT tube. Dilatometer test results are assembled in fig. 4. The indexes proposed for assessing a deposit are plotted from the test results.

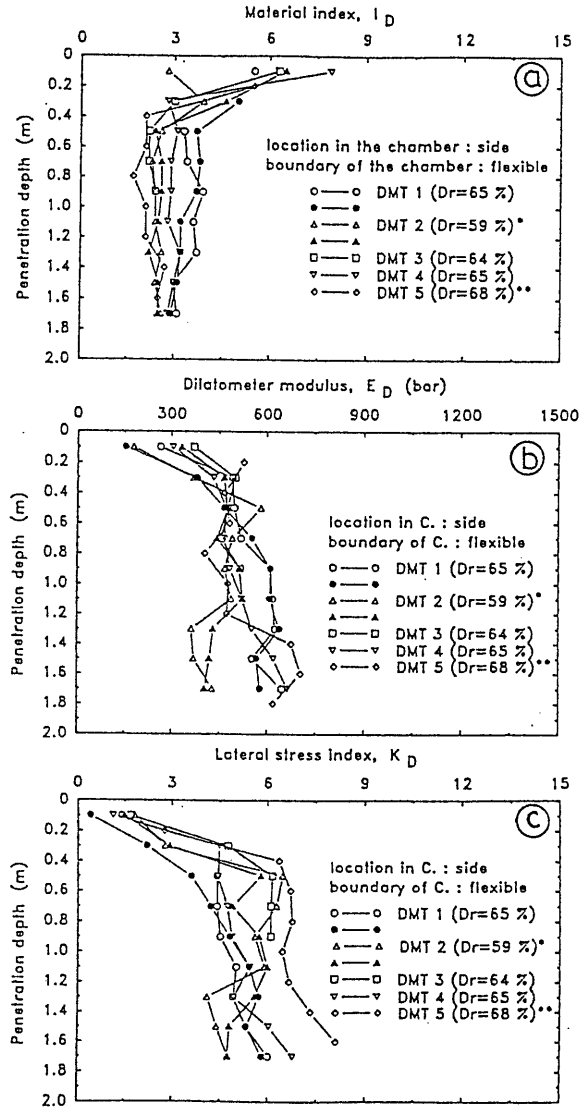

Fig. 4 DMt results

The peak TXC-shear angle of the sand at the test condition was φ = 39° and the maximum shear modulus at very low strain G_{max} = 80 MPa.

Regarding the initial state of the specimen, the uniformity of the specimen can be considered as good both in vertical and lateral direction. However, the stiffness of the specimen is likely to slightly increase with depth. The derived lateral stress coefficient at rest K_0 implies that the specimen is apparently only in a lightly overconsolidated condition, perhaps due to sand tamping in the rigid boundary calibration chamber. Based on many correlations in literature between penetration test results and soil properties, the original strength and deformation properties of the specimen could easily be evaluated for this pure sand, fig. 5.

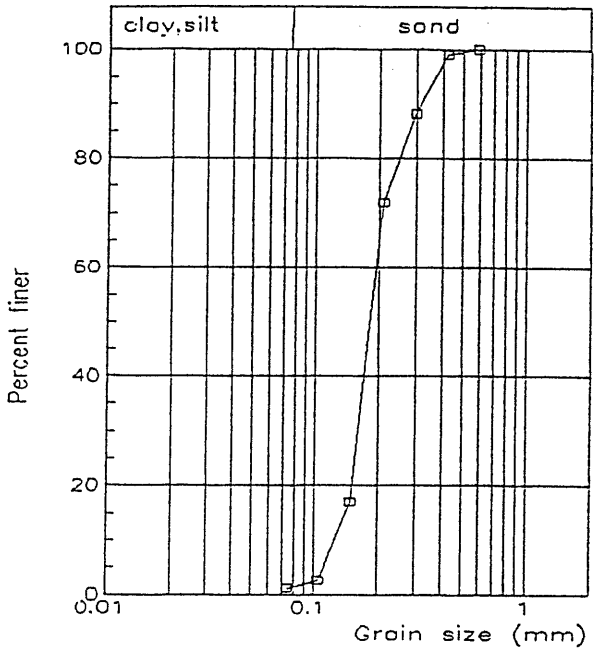

INDEX PROPERTIES OF MOL SAND

Production place	Mol (Belgium)
Mineralogy	quartz
Particle shape	sub-angular
Grain size (mm):	
D_{10}	0.13
D_{50}	0.19
Uniformity coefficient:	
U_c	1.6
Specific gravity: G_s	2.65
Void ratio :	
e_{max}	0.918
e_{min}	0.585
Dry unit weight(kN/m^3):	
γ_{dmax}	16.387
γ_{dmin}	13.553

Fig. 5 Grain size distribution of Mol sand

The model test pile, table 2, carried five load cells at equal interdistance, from top to top. The diameter ratio of chamber to pile became about 40. For the "smooth" pile (S), the stainless steel was left bare ; for the "rough" (R) pile, the shaft was coated with coarse sand.

Table 2 : Model pile properties

Material	Stainless steel
Effective length at initial : l (mm)	1470
Diameter : d (mm)	
smooth pile	35.7
rough pile	40.0
Thickness : t (mm)	
rog segment	10.0
load cell	5.0
Roughness : R_{max} (μm)	
smooth pile	7-10
rough pile	(glued quartz sand)

Regarding the test pile installation and testing procedure three parameters were considered : pile shaft surface roughness (S or R), pile installation method (displacement (D) or buried (ND), fig. 6) and the cyclic load level $\frac{Q_{max}}{Q_{ult}}$, (fig. 7).

(a) Displacement pile

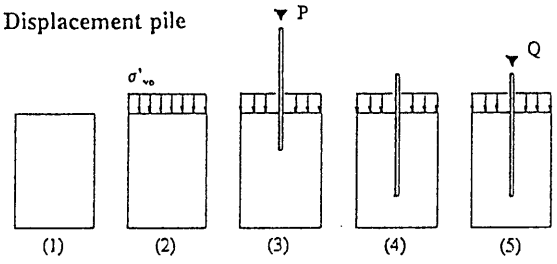

(1) initial deposit
(2) pressurizing (σ'_{vo} = 100 kPa) and stabilizing
(3) pile installation
(4) stabilizing
(5) pile loading :
- initial static loading (1st day)
- cyclic loding (2nd day)
- final static loading (immediatelyafter cyclic loading)

(b) Non-displacement pile (burried pile)

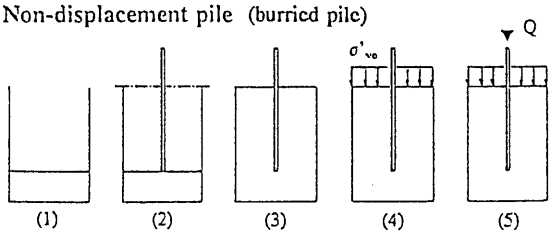

(1) sand bed
(2) pile setup on the sand
(3) initial deposit with pile
(4) pressurizing (σ'_{vo} = 100 kPa) and stabilizing
(5) pile loading :
- initial static loading (1st day)
- cyclic loding (2nd day)
- final static loading (immediatelyafter cyclic loading)

Fig. 6 Test procedure

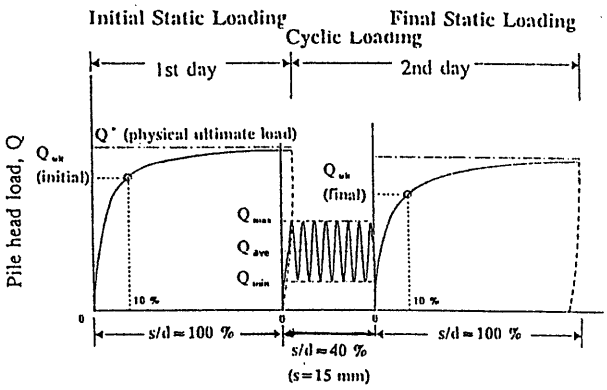

Fig. 7a Sequence of loadings

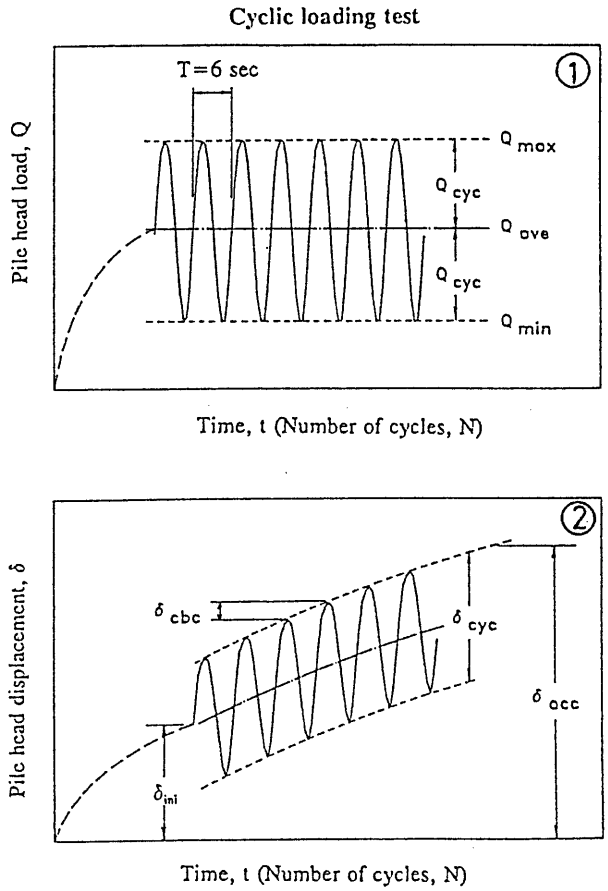

Fig. 7b Test manner and definitions

All loading tests were performed in a load-controled mode. The cyclic loading wave period was set to 6 sec. The summary of the performed pile loading test parameters is given in table 3.

For the interpretation of the test results, the residual locked stresses due to pile installation, especially in the case of displacement piles, were measured before each loading test. Such residual stresses at the pile tip varied typically around 20 kPa for SD, 10 kPa for RD and about 5 kPa for SND piles.

Table 3 : Summary of pile loading test parameters

Test NO.	D_r (%)	Cyclic Loading			
		$\frac{Q_{ave}}{Q_{ult}}$	$\frac{Q_{cyc}}{Q_{ult}}$	$\frac{Q_{max}}{Q_{ult}}$	$\frac{Q_{cyc}}{Q_{ave}}$
RD 1	66	0.40	0.17	0.57	0.43
RD 2	66	0.41	0.22	0.60	0.53
RD 3	67	0.40	0.35	0.76	0.88
RD 4	64	0.40	0.31	0.71	0.77
RD 5	64	0.40	0.40	0.80	0.98
RD 6	62	0.42	0.34	0.76	0.82
RD 7	64	0.40	0.42	0.81	1.05
SD 1	66	0.41	0.31	0.72	0.75
SD 2	67	0.37	0.34	0.72	0.92
SD 3	65	0.37	0.38	0.75	1.04
SD 4	65	0.38	0.27	0.65	0.70
SD 5	66	0.40	0.28	0.68	0.69
SD 6	66	0.42	0.20	0.62	0.48
RND 1	69	0.39	0.40	0.79	1.02
RND 2	68	0.41	0.35	0.76	0.84
RND 3	68	-	-	-	-
SND 2	68	0.37	0.32	0.69	0.87
SND 2	68	0.33	0.40	0.73	1.20
SND 3	68	0.46	0.44	0.89	0.95

TEST RESULTS OF STATIC MODEL PILE LOADING

The static loading test results are gathered in fig. 8 and 9 for the rough and smooth model piles respectively, and summarised in table 4.

Table 4 : summary of static pile load tests in CC.

Pile type	D_r (%)	q_c (MPa)	q_b $\frac{s}{d}$ = 10% (MPa)	q_b $\frac{s}{d}$ = 30% (MPa)	q_b $\frac{s}{d}$ = 100% (MPa)	f_s $\frac{s}{d}$ = 10% (KPa)	f_s $\frac{s}{d}$ = 100% (KPa)
RD	65	11	11.3	12.2	12.4	156	135
SD	66	12	9.9	10.6	11.4	61	65
RND	68	13.5	3.1	4.6	7.3	106	92
SND	68	13.5	2.5	3.6	5.6	32	31

The unit toe resistance q_b at s/d = 10 %, 30 % and 100 % are not surprisingsly very much in accordance with the relevant q_c values. On the other hand, the q_b value for non-displacement (buried) pile still heavily depends on the settlement level even after the conventional s/d = 30 % - value. These observations coincide with many experimental test results both in model and prototype piles.

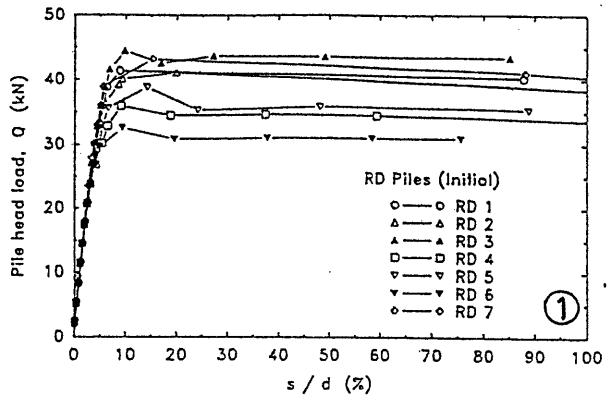

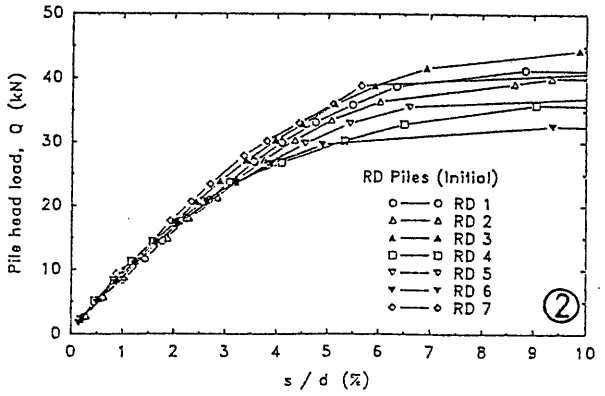

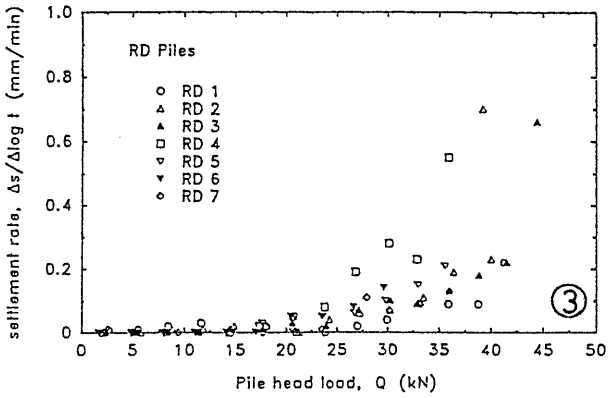

Symbol	○	△	▲	□	▽	▼	◇
D_r (%)	66	66	67	64	64	62	64

Fig. 8a Load settlement - rough, displacement (RD) pile

The rough piles show a peak value for the unit shaft resistance at about 10 % of the relative settlement, whereas it is not clear at all for the smooth piles, due to interface slip.

Intuitively, the observed pile shaft behaviour is similar to the interface simple shear test results when implementing different roughnesses of the shaft. For the RD piles, a clear peak appears at much larger displacement with much higher shear resistance than for SD piles. For SD piles, the unit shaft resistance is abruptly flattened due to the interface slip.

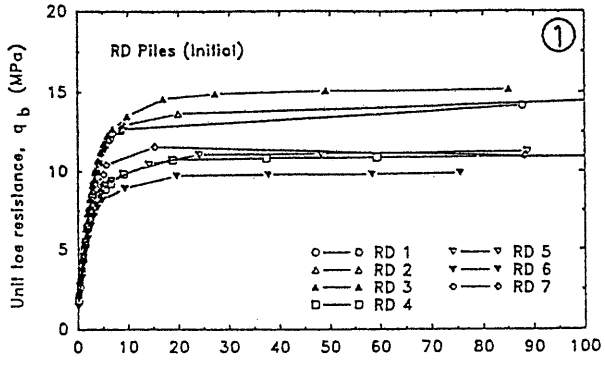

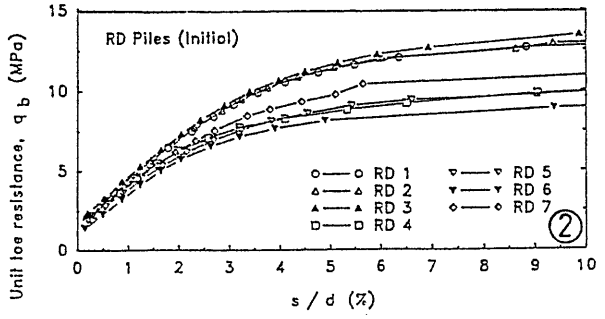

Symbol	○	△	▲	□	▽	▼	◇
D_r (%)	66	66	67	64	64	62	64

Fig. 8b Unit toe resistance - settlement - rough, displacement (RD) pile

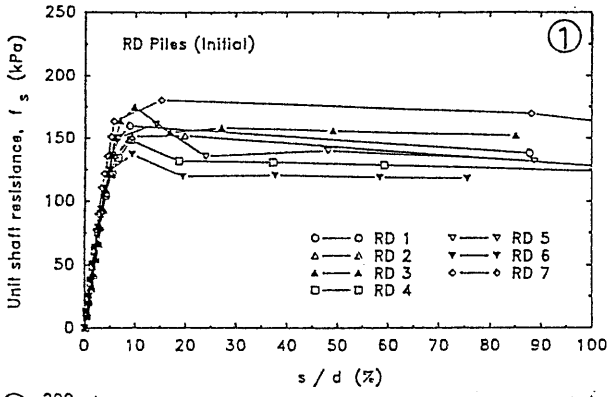

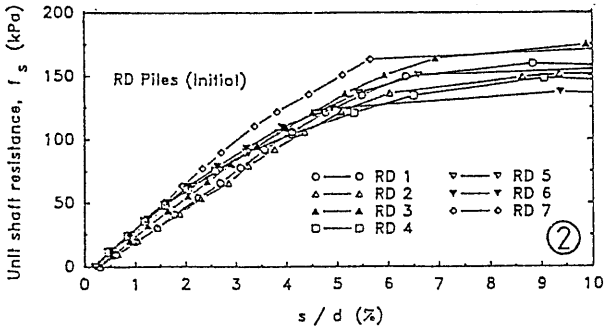

Symbol	○	△	▲	□	▽	▼	◇
D_r (%)	66	66	67	64	64	62	64

Fig. 8c Unit shaft resistance - settlement rough, displacement (RD) pile

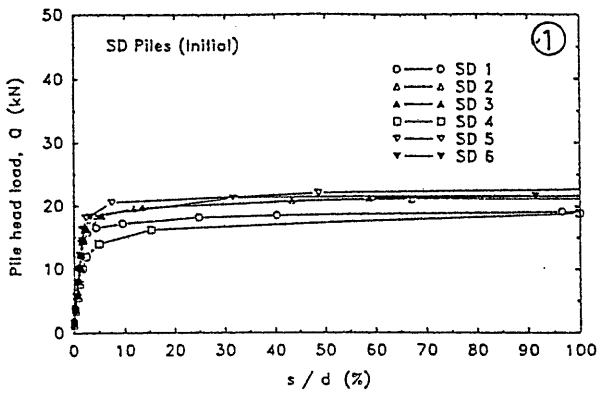

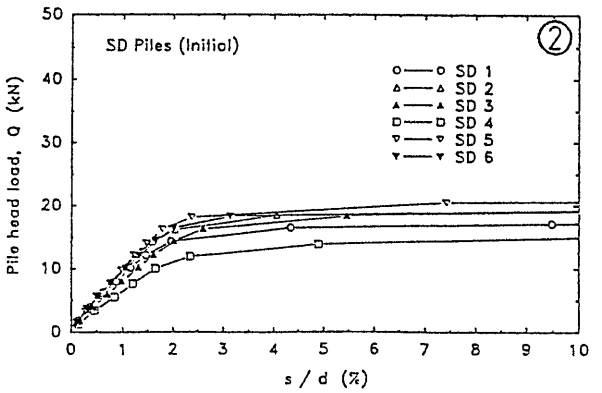

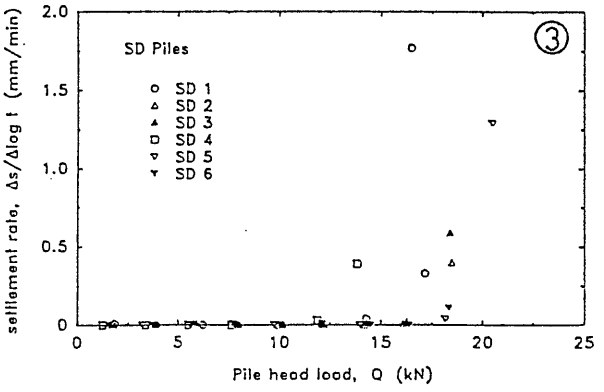

Symbol	○	△	▲	□	▽	▼
D_r (%)	66	67	65	65	66	66

Fig. 9a Load settlement smooth, displacement (SD) pile

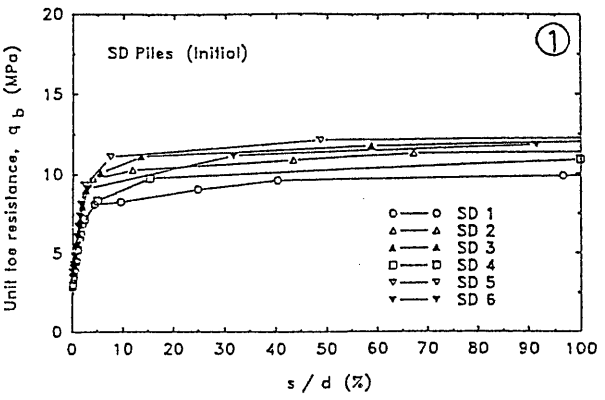

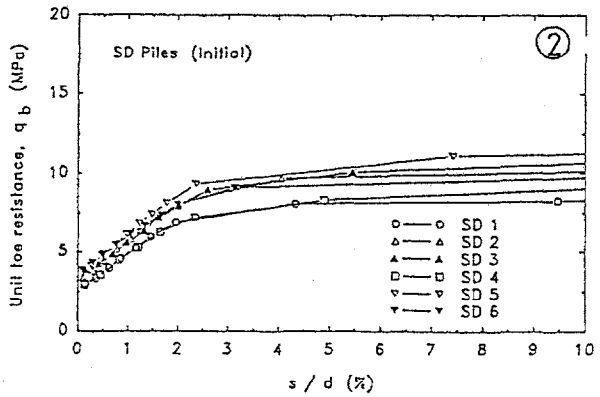

Symbol	○	△	▲	□	▽	▼
D_r (%)	66	67	65	65	66	66

Fig. 9b Unit toe resistance - settlement smooth, displacement (SD) pile

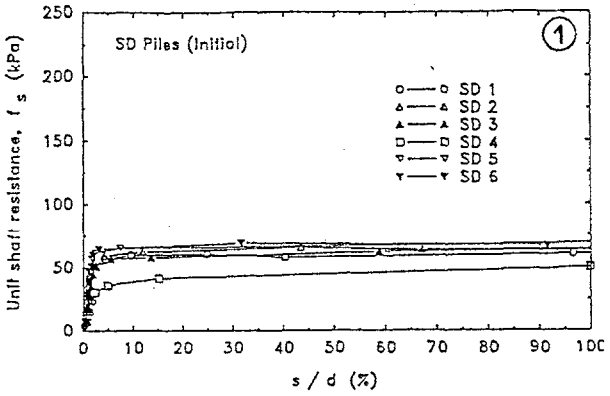

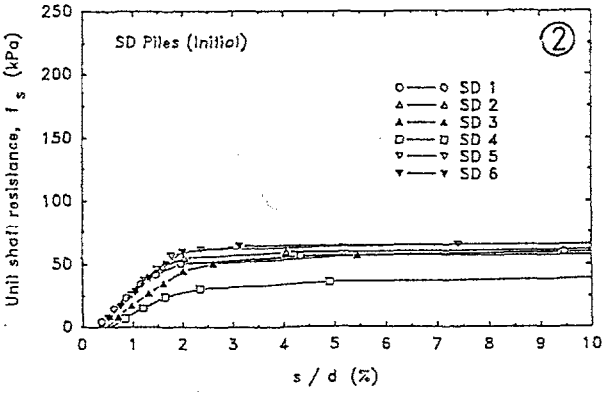

Symbol	○	△	▲	□	▽	▼
D_r (%)	66	67	65	65	66	66

Fig. 9c Unit shaft resistance - settlement smooth, displacement (SD) pile

TEST RESULTS OF THE CYCLIC LOADING ON THE MODEL PILES

Referring to the fig. 7b and the table 3 data, the most interesting picture of the cyclic load settlement behaviour is coming from the analysis of the cycle-by-cycle pile head displacements (δ_{cbc}). The (δ_{cyc}) one-cycle-displacement (fig. 7b) as a function of the "cyclic stiffness" of the model-pile soil system. From the results on fig. 10, it can be derived that in our tests this "cyclic stiffness" is equivalent to about 25 kN/mm, which is in agreement with the initial static pile load-settlement stiffness (fig. 8 and 9). For RD piles, the cycle by cycle displacement (fig. 11) steadily decreases with cycles up to a certain number of cycles depending on the applied cyclic load level. If the applied cyclic load is considerably large, the cycle-by-cycle displacement only over a few cycles slightly decreases, whereafter it increases drastically. This figure strongly reflects a soil "creep" behaviour for a pile behaviour under one-way cyclic loading, in clay soils.

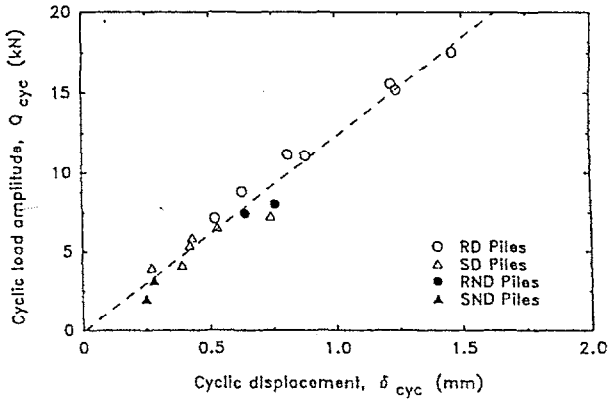

Fig. 10 Cyclic load - Cyclic displacement

As expected, a very different behaviour comes out from the SD pile tests (fig. 12). Although a drop of the cycle-by-cycle displacement occurs occasionaly at the beginning of the loading, it mostly increases steadily.

If the pile behaviour is predominantly governed by the lateral stresses acting on the pile shaft, we can anticipate some changes of the shaft resistance during cyclic loading (fig. 13 a,b). The figures indicate the unit shaft resistance in the upper half of the pile, varying with the accumulated displacement.

Under a highenough cyclic loadlevel, the unit shaft resistance for RD-piles increases up to 4-5 mm of overall settlement, then gradually decreases with increasing displacement. On the contrary, under a lower cyclic load, the unit shaft resistance drops clearly at the beginning depending on the cyclic load level, followed by a slight recovery, the shaft resistance becoming almost constant at the end.

The SD-piles' unit shaft resistance drops in all cases particulary at the beginning of the loading, then tends towards or stable position. Both the unit toe resistance and the unit shaft resistance before cyclic loading and after cyclic loading are compared in figure 14.

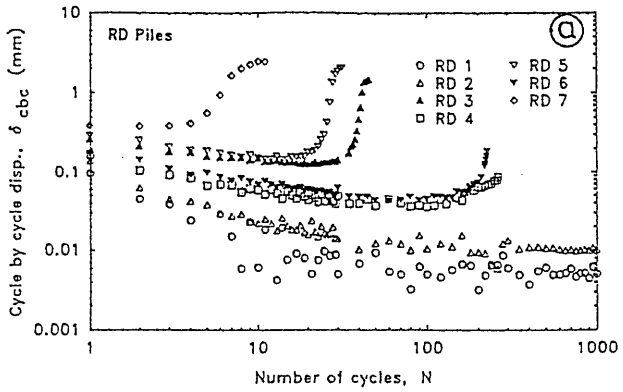

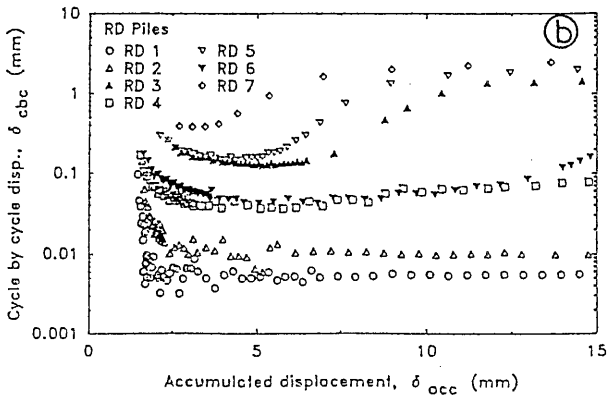

Symbol	◇	▽	▲	▼	□	△	○
$\frac{Q_{max}}{Q_{ult}}$	0.81	0.80	0.76	0.76	0.71	0.60	0.57
$\frac{Q_{cyc}}{Q_{ave}}$	1.05	0.98	0.88	0.82	0.77	0.53	0.43

Fig. 11 Cycle by cycle displacement rough, displacement (RD) pile

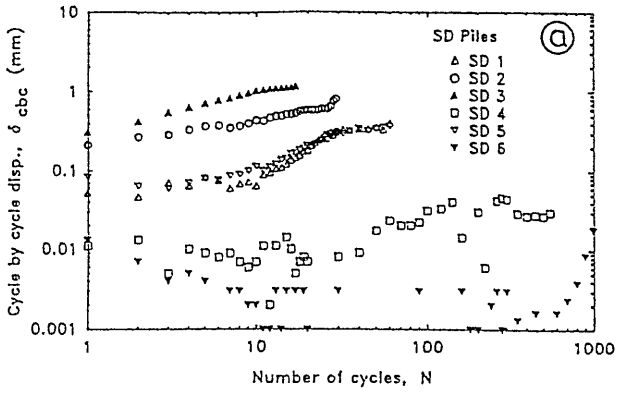

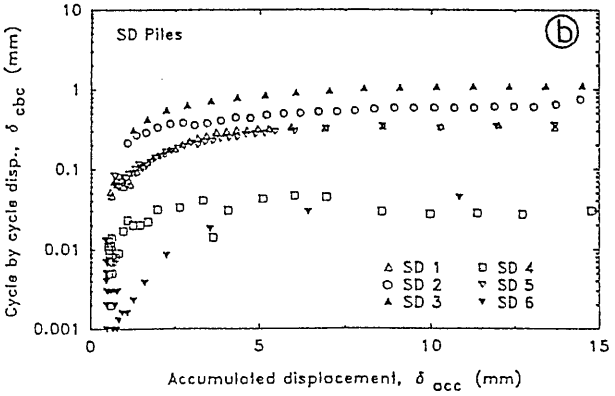

Symbol	▲	○	△	▽	□	▼
$\frac{Q_{max}}{Q_{ult}}$	0.75	0.72	0.72	0.68	0.65	0.62
$\frac{Q_{cyc}}{Q_{ave}}$	1.04	0.92	0.75	0.69	0.70	0.48

Fig. 12 Cycle by cycle displacement smooth, displacement (SD) pile

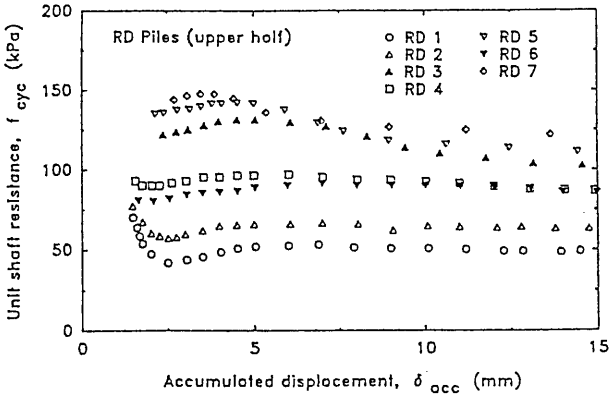

Symbol	◇	▽	▲	▼	□	△	○
$\frac{Q_{max}}{Q_{ult}}$	0.81	0.80	0.76	0.76	0.71	0.60	0.57
$\frac{Q_{cyc}}{Q_{ave}}$	1.05	0.98	0.88	0.82	0.77	0.53	0.43

Fig. 13a Cyclic unit shaft resistance rough, displacement (RD) pile

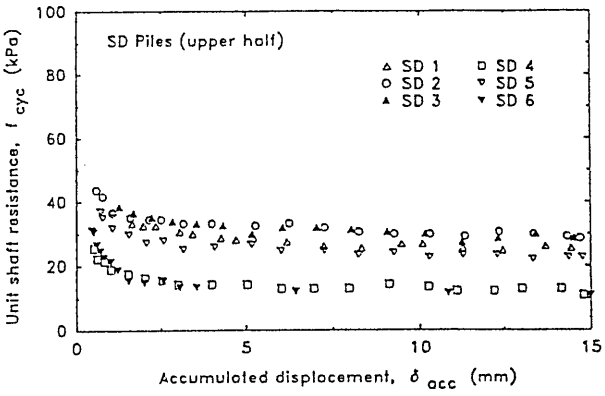

Symbol	▲	○	△	▽	□	▼
$\frac{Q_{max}}{Q_{ult}}$	0.75	0.72	0.72	0.68	0.65	0.62
$\frac{Q_{cyc}}{Q_{ave}}$	1.04	0.92	0.75	0.69	0.70	0.48

Fig. 13b Cyclic unit shaft resistance smooth, displacement (SD) pile

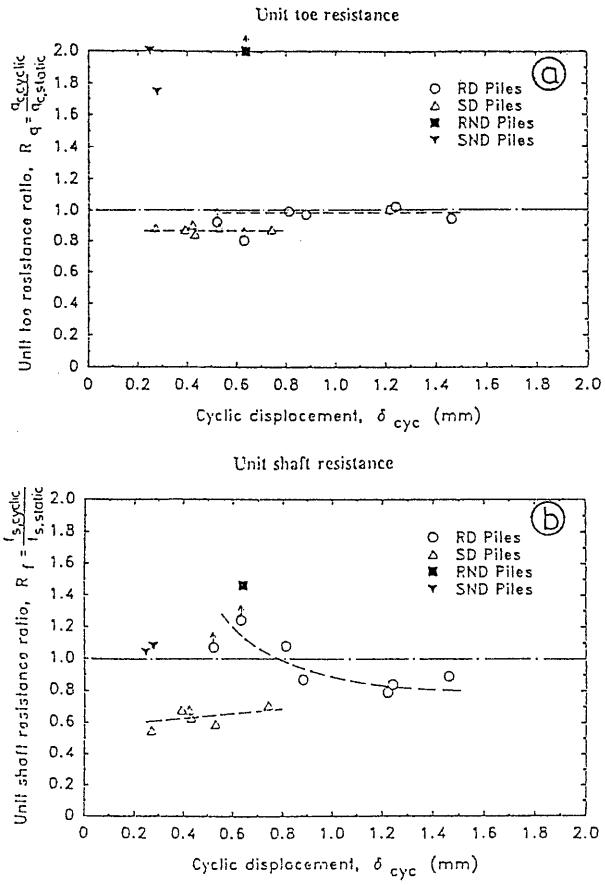

Fig. 14 Influence of cyclic loading history on static resistance

Regarding the unit base capacity, almost no influence of static preloading for RD piles is measured, while q_b is only slightly degraded for SD piles. On the contrary q_b increases dramatically for buried piles, because of strong settlement dependency of q_b and some compaction effect underneath the pile toe in this type of pile installation.

With respect to the unit shaft resistance, the ratio of resistance before and after cyclic loading depends on the applied cyclic load level on the RD pile. Under a large cyclic load level the static f_s, is finally degraded. On the contrary, applying a small cyclic load level on RD piles is preferable to gain shaft resistance. For SD piles, the unit shaft resistance is severly degraded in all cases. The combination of the particle re-orientation and some interface slip finally destroys the SD pile shaft capacity.

CONCLUSIONS

There is an analogy between the simple qualitative displacement model pile behaviour under one-way cyclic loading in sand and soil "creep" behaviour. Similar behaviour trends as wellknown for RD piles in clayey soils are such behaviour can be attributed to the internal change of the sand fabric in the immediate surrounding of the model pile, during cyclic load regardless of the pile roughness and installation method, the cyclic "critical" load corresponding to the turning point of the δ_{cbc} diagram under a one-way cyclic loading, ranges from 70 to 80 % of the static conventional ultimate capacity. This observation for sands also coincides with the previous cyclic pile test results in clayey soils.

REFERENCES

1. GHIONNA V.N, JAMIOLKOWSKI M., LANCELOTTA M. and PEDORONI S. Base capacity of bored piles in sands from in situ tests. Proceeding 2nd Int. Seminar for Deep Foundations on Bored and Auger Piles, 1993, Ghent, Belgium , pp. 67-76.

2. INA K., UESUGI M. and KISHIDA H. Displacement of single floating piles under cyclic axial loads in clay. 1993, to be published in ASCE.

3. KANAI S. An Experimental Study on Model Pile Behaviour under Cyclic Loading in Sand. 1993, PhD, Ghent University, Belgium

4. KORECK H.W. and SCHWARTZ P. Axial cyclic loaded piles. Proceeding 1st Int. Seminar for Deep Foundations on Bored and Auger Piles, 1993, Ghent, Belgium, pp. 395-399.

5. MURAYAMA S., MITCHHIRO K. and SAKAGAMI T. Creep characteristics of sands. Soils and Foundations 1984, vol. 24, No 2, pp. 1-15.

6. POULOS H.G. Cyclic axial loading analysis of piles in sand. J. Geotech. Engineering Div., ASCE, 1989, Vol. 115, No GT6, pp. 836-852.

7. RANDOLPH M.F. Capacity of piles driven into dense sand. Cambridge Univ. Engineering Report, 1985, UK.

8. UESUGI M. AND KISHIDA H. Discussion for Cyclic axial loading analysis of piles in sand. J. Geotech. Engineering Div. ASCE, 1990, Vol. 117, No GT9, pp. 1435-1439.

9. VAN IMPE W.F. Developments in pile design. Proceeding 4th International Conf. on Piling and Deep Foundations, 1990, Stresa, Italy.

10. VAN IMPE W.F. Deformation of deep foundations. Proceeding 10th ECSMFE, 1991, Florence, Italy.

11. VESIC A.S. Ultimate loads and settlement of deep foundations in sand. Proceeding of Symposium held in Druke University, 1965, USA.

12. YABUUCHI S. and HIRAYAMA H. Bearing mechanisms of nodal piles in sand. Proceeding 2nd International Seminar for Deep Foundations on Bored and Auger Piles, 1993, Ghent, Belgium, pp. 333-336.

13. YOON Y. Static and Dynamic behaviour of crushable and non-crushable sands, 1991, Ph. D. Thesis, Ghent University, Belgium.

DFI 94

FIFTH INTERNATIONAL CONFERENCE AND EXHIBITION ON PILING AND DEEP FOUNDATIONS

13 - 15 June 1994

Belfry Hall • Bruges • Belgium

The Sponsors

Co-Sponsors

EUROPEAN FEDERATION OF FOUNDATION CONTRACTORS (EFFC)

INTERNATIONAL SOCIETY FOR SOIL MECHANICS & FOUNDATION ENGINEERING (ISSMFE)

TECHNICAL EUROPEAN SHEET PILING ASSOCIATION

DFI 94 Conference and Exhibition has been organised on behalf of the Sponsors and Co-Sponsors by their appointed organisers, Westrade Fairs Ltd.

WESTRADE FAIRS LTD
28 Church Street
Rickmansworth
Herts WD3 1DD • UK
Tel: +44 (0)923 778311 Fax: +44 (0)923 776820